LAWRENCE
LIVERMORE
NATIONAL
LABORATORY

LLNL-TR-680742

An Investigation on X-ray Reflectivity technique at LLNL

C. K. Saw, W. K. Grant, J. Stanford, L. N. Dinh

January 12, 2016

Disclaimer

This work performed under the auspices of the U.S. Department of Energy by Lawrence Livermore National Laboratory under Contract DE-AC52-07NA27344.

An Investigation on X-ray Reflectivity technique at LLNL

C. K. Saw, W. K. Grant, J. A. Stanford and L. N. Dinh
Lawrence Livermore National Lab., Livermore, CA 94551

Abstract

X-ray reflectivity (XRR) is a non-contact, non-destructive technique used to measure the near-surface structure of many materials. It probes the electron density contrast with depth resolution of less than one nm to several hundreds of nm. As a consequence, it gives information on the roughness and thickness of the thin film formed on a wafer substrate or bulk surface. These films can be oxides, polymer coatings, ceramics or metals and they can be crystalline or non-crystalline in nature.

This report documents the work carried out to determine the feasibility of using this technique for Pu oxide grown on bulk Pu system. It also provides the experimental and theoretical considerations in carrying out XRR technique to determine film thicknesses. The intention of this work is to develop the methodology and understand the limits for carrying out such experiments using the in-house technique.

Our results indicate that meaningful XRR spectrum can be acquired on test samples of SiO_2 on Si wafer and Ta_2O_5 on bulk Ta. The thicknesses derived here are consistent with that measured with UV-Vis (ultra-violet/visible) spectroscopy. However, in the case of Pu oxide formed on Pu surface, our result did not show the presence of multiple fringes and upon further electro-polishing, only two were observed. Based on the 2 fringes, the oxide thickness calculated was not consistent with that observed by SEM images. This was caused by significant amount of diffuse scattering due surface and interface roughness. As verified by SEM images, this surface was laden with protrusions and upon being electro-polished, developed significant numbers of "valleys" and "hill".

Several factors contribute to the quality of XRR spectrum. However, surface roughness is most destructive for the success of XRR technique. Simulation of PuO_2/Pu also proves that the surface and interface roughness of merely 2 nm can adversely affect the quality of the spectra. Furthermore, due to instrumental resolution, this technique is ideal only for thicknesses of less than 50 nm.

I. Introduction:

Fundamentally, XRR measures the interference of the reflected x-ray from two planes, the surface due to total external reflection and interface, between the film and the substrate as a result of combination of reflection and refraction processes. In order to achieve sufficient scattered signals, the sample area and the beam flux need to be large. Moreover, the beam has to be very well collimated as well since the scattering angle is only a few degrees in 2θ and the oscillations can be very small. For these reasons, most of the reflectivity experiments are carried out at synchrotron sources. Unfortunately, this is not often possible due to the difficulties in securing and handling of Pu samples. An in-house capability is clearly desirable.

Our recent purchase of the in-house Rigaku Smartlab X-ray System has the XRR capability built in. It uses the latest technology in Gobël mirror to condition the diverging beam from the x-ray tube to a highly confined parallel beam, which is then further slit down to only a few microns thick and 5 mm wide. The beam thickness defines the instrumental resolution which is required for XRR experiments, especially thick surface layer.

The basic principle of XRR [1] is shown in Figure 1. Essentially, the specular reflection from the flat surface is measured. If the incident beam is below the critical angle, the x-rays will be totally external reflected. If the incident beam is above the critical angle, some of the photons will penetrate the sample via the process of refraction due to the differences in densities while some will be reflected at the surface. The refracted beam will again interact at the interface and be totally reflected back and out of the sample. The conditions for reflection and refraction clearly depend on electronic densities of the different film layers which are related to differences of the reflective indexes. It is the interference of the wave from these two planes that generates the fringes which contain information on the thickness and the roughness of the layers.

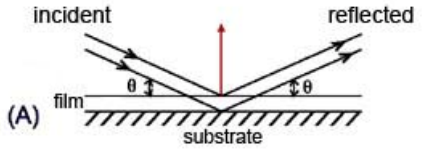

Figure 1: Schematic of the experimental setup

In the classical formalism, the reflective index is given as

$$n = 1 - \delta + i\beta \tag{1}$$

where δ and β represent the dispersion and absorption factors, respectively, and are given by:

$$\delta = \frac{r_o \lambda^2}{2\pi} (Z + f').n_{Atom} \tag{2}$$

$$\beta = \frac{r_{o\lambda^2}}{2\pi} f".n_{Atom} \tag{3}$$

The electron density is given as $Z.n_{Atom}$ where Z is the atomic number and $n_{Atom} = N_A.\ \rho/A$, N_A is the Avogadros number and A is the atomic weight. r_o is the Bohr radius and f' and f'' are the dispersion factors. λ is the wavelength of the radiation. Hence, it can be observed that δ and β are related to the density and absorption of the film, respectively. Typically, δ is in the order of 10^{-5} and β in the order of 10^{-8}. Assuming when there is no absorption (below and at the critical angle), the critical angle can be expressed as,

$$\theta_c = \sqrt{\frac{r_{o\lambda^2}}{\pi}}\rho \tag{4}$$

Therefore, the density can be extracted from the location of the critical angle. Above the critical angle, Kiessig fringes [2] are formed due to the interference of the two waves and they are given by

$$\theta_m^2 - \theta_C^2 = m^2 \frac{\lambda^2}{4d^2} \tag{5}$$

where m is the m^{th} oscillation, θ_C^2 is the critical angle and as a consequence, when m equals to 1 (1^{st} order peak), the thickness τ can be written as,

$$\tau = \frac{\lambda}{2\Delta\theta} \tag{6}$$

where $\Delta\theta$ is the distance between 2 oscillations, λ is the x-ray wavelength.

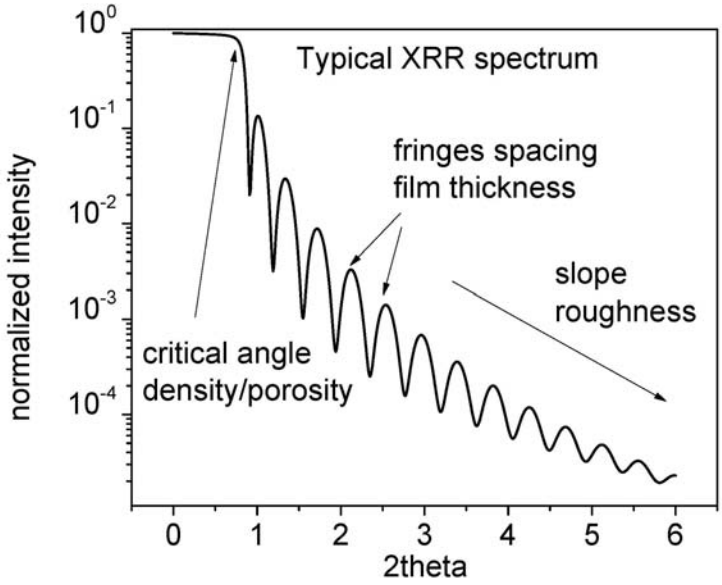

Figure 2: Schematic diagram of typical XRR spectrum

Typical curve derived from an XRR experiment is shown in Figure 2 and it consists of very high intensity at very low angle and very low intensity at high angle. Data are collected as a function

of scattered angle 2θ from the surface. The scattering angle is typically <10º (2θ) for wavelength of 1.54 A or energy of 8.04 KeV. As stated earlier, the decay of the specular reflection goes as Q^{-4} (A^{-1}), where $Q=4\pi \sin(\theta)/\lambda$. Q is refers to as scattering vector. For that reason, the plots are given with log scale on the y axis versus angle 2θ (or Q) on the x axis.

The density can be calculated from the location of critical angle by using equation (4) as indicated in the plot. The spacing of the oscillations gives rise to the thickness of the film. The amplitude of the oscillation gives information on the densities contrast at the interface and the decay of these oscillations signifies the roughness.

I. Factors affecting the XRR technique

Theoretical simulation to generate the XRR spectrum is quite well understood which requires a complex recursion formula [1, 2]. Routines for such simulation are freely available [3, 4]. For the present simulation, Global Fit routine from Rigaku Corp. is used. This simulation requires the knowledge of the densities, estimated thicknesses and roughness.

(a) Density contrast

Figure 3 is an example which compares the calculations of the change in fringe magnitude with densities contrast for SiO_2, Ni and Au on silicon wafer. The calculation is based on a 20 nm thick layer. SiO_2 has a density of 2.2 gm/cc and Si has a density of 2.329 gm/cc. This contrast is very small when compares to Ni (8.9 gm/cc) or Au (19.3 gm/cc) on Si substrate. Since, the magnitude of the fringes for SiO_2 is relatively small, data acquisition for such a system is more difficulty.

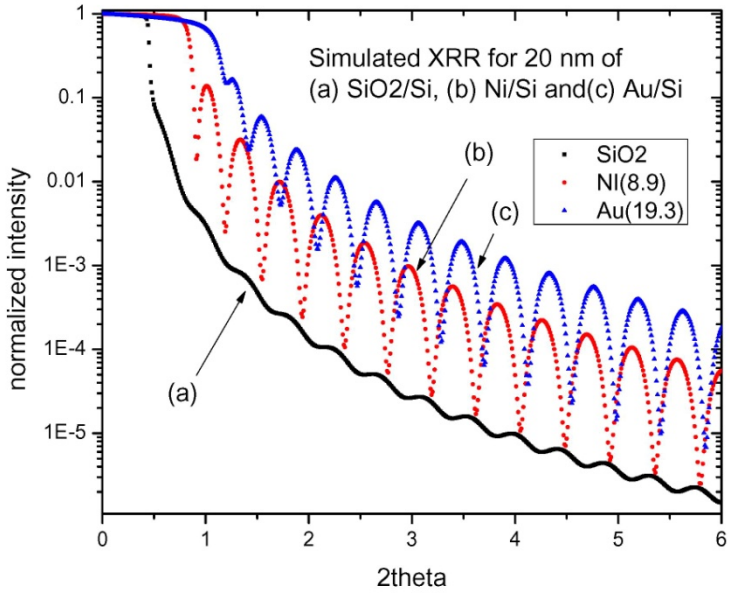

Figure 3: Comparison of magnitudes of fringes for different density ratios

(b) Roughness

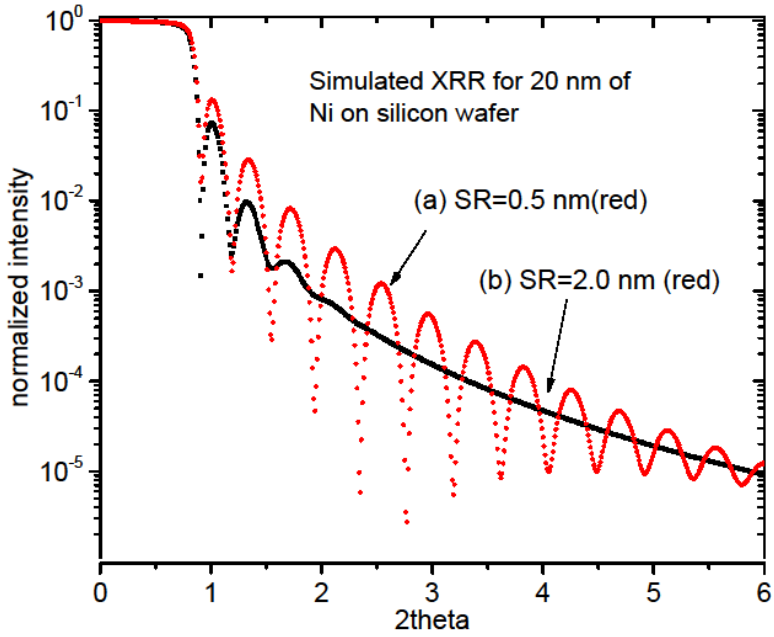

Figure 4: Simulated spectra for Ni/Si with different surface roughness

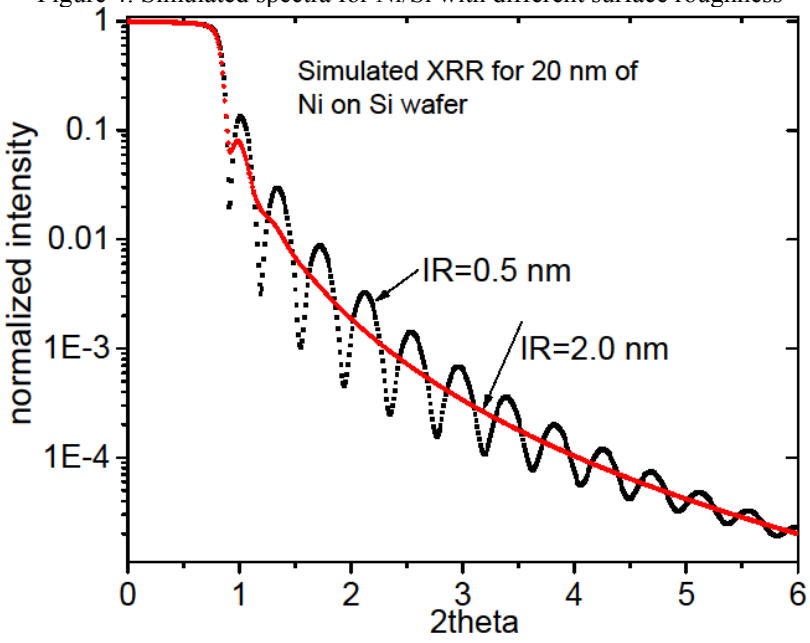

Figure 5: XRR spectrum with different interface roughness

Surface roughness also greatly affects the quality of the XRR spectra. There are two roughness components, the surface (SR) and interface roughness (IR). The SR is associated with the surface of the film while the IR is between the substrate and the film. As an example, as shown in Figure 4 for a simulation of 20 nm thick Ni on silicon wafer substrate, the surface roughness of only 2 nm, as shown by the black curve, clearly diminished significantly the magnitude of the fringes at high angle when compared to the spectra with surface roughness of 0.5 nm as indicated by the red curve. The black curve flattens out after 3 fringes. Figure 5 compares similar XRR calculation with differences in the interface roughness (IR). Again, as it can be observed, the magnitude of the fringes drastically reduced with merely 2 nm IR.

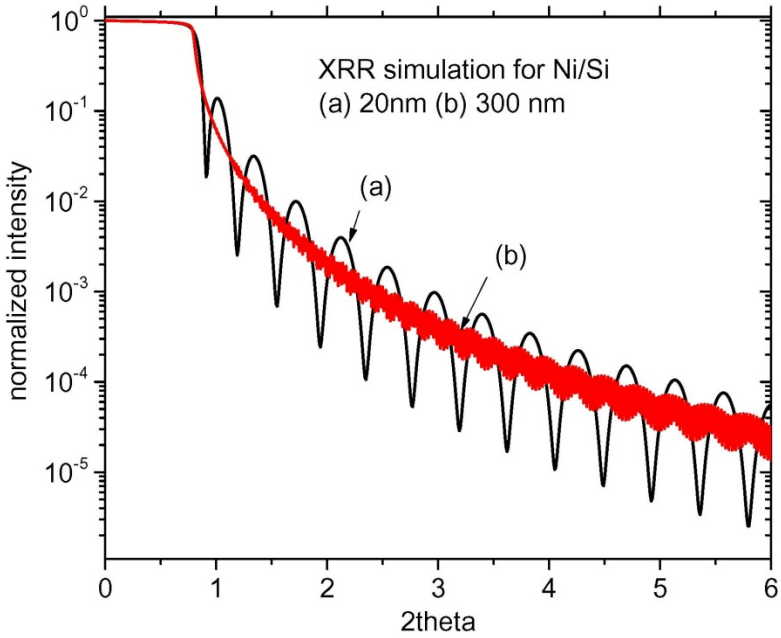

Figure 6: XRR fringes as a function of film thickness for Ni on silicon wafer.

(c) Film thickness

The measurement of the fringes also greatly depends on the inherent instrument resolution which is directly correlated to the x-ray optics, and the ability to differentiate x-ray scattered at very close angle with each other. For example, for Ni film deposited on silicon wafer and with a thickness of 300 nm, the expected XRR fringes collapse into very closely packed in 2θ, which makes detection very difficult especially when the instrument resolution is wider than the width of the fringes as shown in Figure 6.

(d) Absorption

It can also be explained that the atomic number of the material contributes to the quality of the formation of the fringes. For x-rays, the absorption factor is directly correlated with atomic number. The higher the atomic number, the higher the absorption which means that there are less x-ray coming out from the sample to form fringes. The absorption problem is only critical at very low angle. This will be further explained in the later section.

(e) Reduced irradiated sample area with angle

This issue refers to the area sampled by the x-rays as a function of angle. Typically, this is not a factor in conventional x-ray diffraction technique since the beam height can be as large as 1 mm which is much larger than what is required in an XRR experiment. Moreover, focusing and compensating slits have been introduced to maintain equal irradiated surface area at all scattering angle. In XRR technique, however these additions are not viable. Therefore, the area irradiated by the x-rays will be reduced greatly with increasing scattering angle.

II. Experimental

The Rigaku SmartLab X-ray System is located in B331. The diverging beam from the x-ray tube is made into a parallel beam with a Globel mirror. This is a very important component of an XRR instrument as well as the ability to perfectly align the sample surface parallel to the beam. The instrument also has the ability to make very small angular steps of 0.001° (2θ). Apart from the θ and 2θ movements, the diffractometer also has the χ and φ movements. χ rotation is about the scattering plane and φ axis is about the sample surface plane. The beam is set to be about 5 mm wide and 16 μm height to cover the surface of the 5/8" diameter sample disk at low angle.

Two types of samples were selected as test samples for this investigation (a) oxide on Si wafer and (b) oxide generated from a clean polished Ta bulk metal surface for the test experiments. Si wafer is commercially available and is known to have a few nm thick of silicon oxide. Both samples were kept at roughly an area of 5/8" square. The Ta sample was mechanical polished with ½ micron slurry.

For Pu sample, it was also mechanically polished, cleaned and loaded onto a special air sensitive holder to prevent further oxidation. The sample was also further polished with ¼ μm diamond solution and then electro-polished to remove the protrusions found on the surface.

(a) Wafer samples

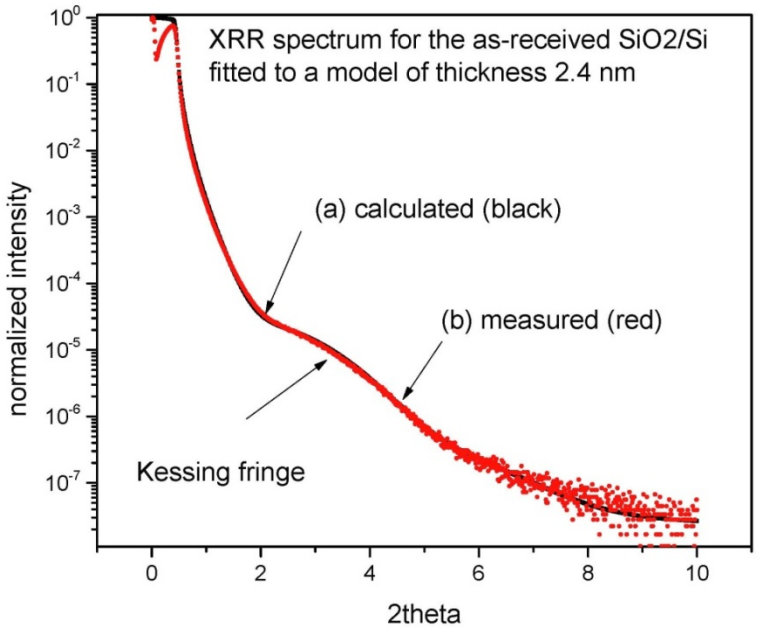

Figure 6: XRR spectrum fitted using Global Fit

As a test of principle, XRR experiment was carried out to determine the SiO_2 thickness on a 2 inch diameter Si wafer. Typically the as-received silicon wafer is considered to be extremely flat and has an oxide layer of a few nm. Figure 6 shows the resulting reflectivity measurement from

the wafer. Even though only one fringe can be observed, the analysis is carried out using a profile fitting routine (Rigaku Global Fit) which indicates that the oxide thickness is ~ 2.4 nm as expected. This thickness was later confirmed using UV-Vis spectroscopy which indicates an oxide thickness between 2~6 nm.

Another test of principle was carried out by performing similar experiment on a thicker oxide wafer sample than the above sample. The oxide layer was grown by heat treating the wafer at 1000ºC for 1 to 2 hours. The XRR spectrum is shown in Figure 7. Multiple fringes can be clearly observed and the result from the fitting routine suggests that the oxide layer is 28 nm. This oxide thickness was also checked to be ~27 nm by the well calibrated UV-Vis spectrometer.

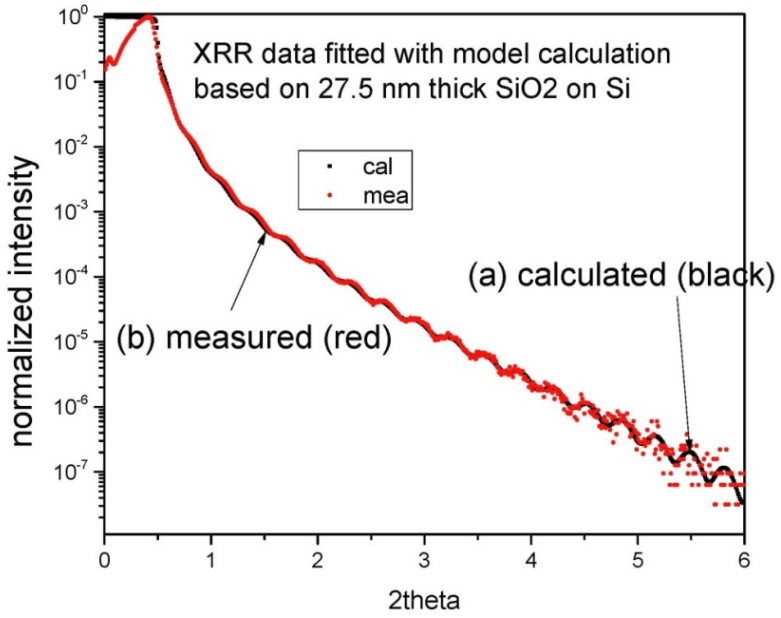

Figure 7: XRR spectrum for annealed SiO_2 on Si

(b) <u>Bulk sample</u>

In order to carry out XRR measurements on our Pu samples, a test experiment was carried out on the oxide formed on bulk Ta sample rather than on a wafer. The sample was ~½ inch diameter disk and a few mm thick. The native oxide build up on a freshly polished surface is normally a few nm depending on the elemental purity, cleanliness, roughness and etc. The resultant XRR spectrum for bulk Ta is shown in Figure 8. Interference fringes can be observed and the result can be fitted to a model of oxide thickness of 2.2 nm, indicating that the oxide from bulk surface can also be measured. The resultant thickness derived here is very reasonable. In order to observe XRR spectra from Ta sample, presumably the IR and SR have to be below 2 nm. No further investigation was carried out since this was not the focus of our present work.

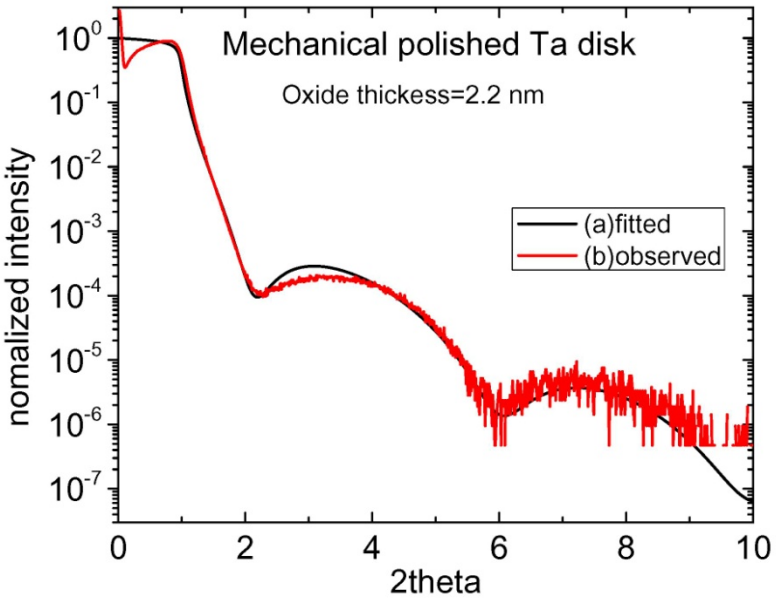

Figure 8: XRR spectrum from polished bulk Ta disks

(c) Plutonium bulk sample

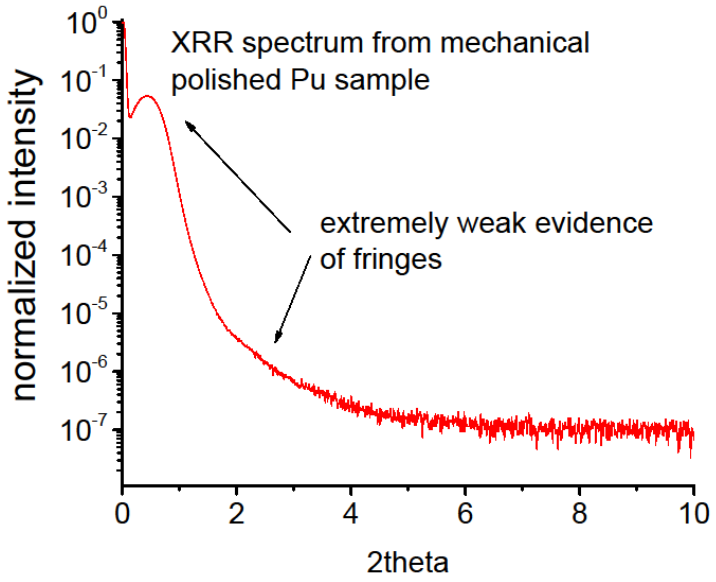

Figure 9: XRR spectrum from mechanical polished Pu surface

Since Pu oxidized readily, Pu surface had to be prepared in a special way in the glove box filled with an inert atmosphere. The sample was polished to a good finish with ¼ micron diamond paste on a micro cloth. The sample disk was about 5/8" in diameter. It was then encapsulated in a special air sensitive Bruker holder to avoid radioactive contamination of the air and further oxidation of Pu by air. The XRR result is shown in Figure 9. Clearly, no fringes are observed. This lack of fringes was probably due to sample roughness. So, SEM image of the sample was acquired and shown in Figure 10 which clearly reveals "protrusions" or "hill". These protrusions were due to mixed phases and segregations of alloys of iron, confirmed by elemental analysis.

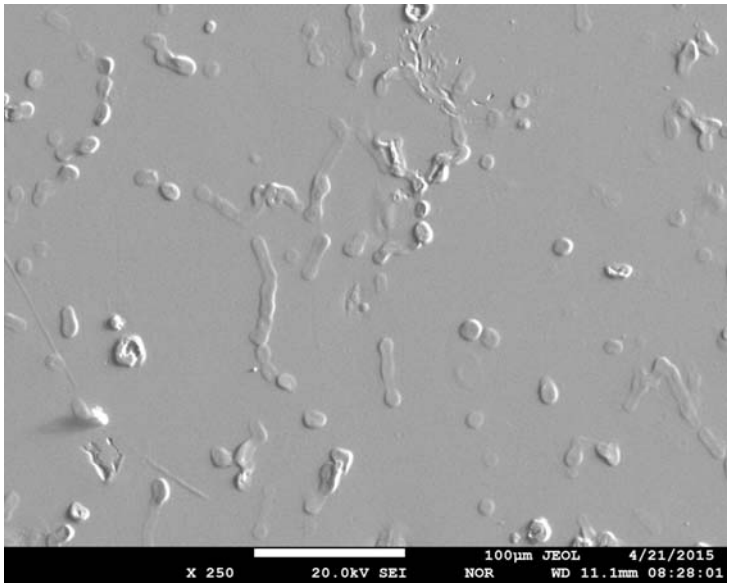

Figure 10: SEM picture of mechanical polished Pu surface showing the protrusions

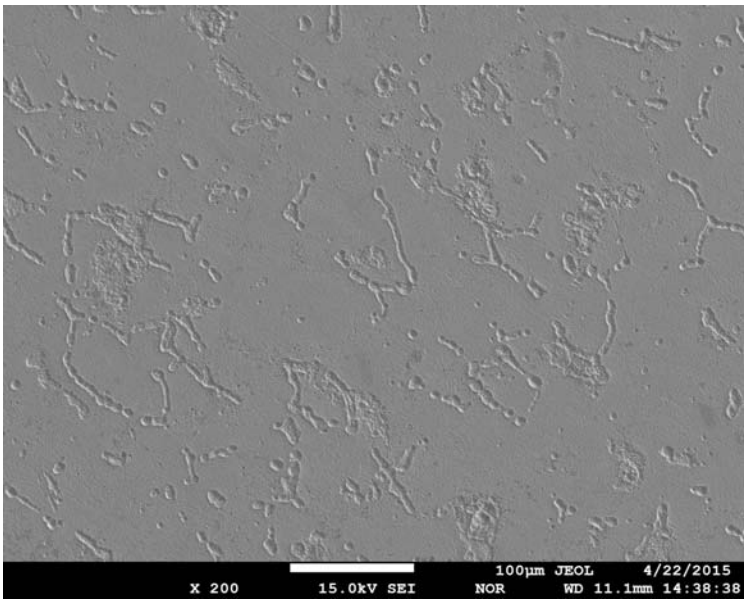

Figure 11: XRR of electro-polished Pu sample

The sample was further electro-polished by dissolving areas that were susceptible to chemical attack. The resulting SEM image is shown in Figure 11 which indicates a drastic improvement in the smoothness of the sample. The protrusions were clearly removed.

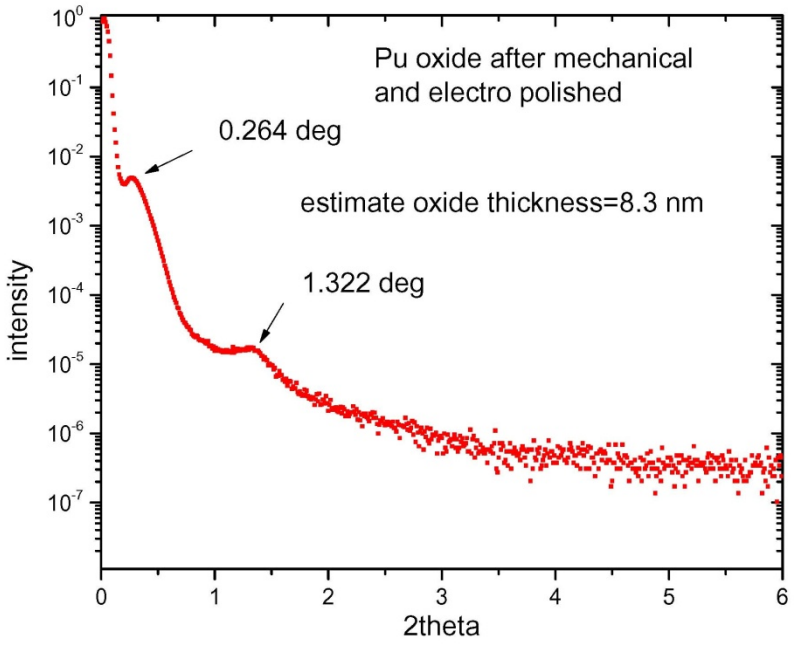

Figure 12: XRR spectrum for Pu after electro-polishing.

The resultant XRR spectrum for the electro-polished is shown in Figure 12. Unlike previous scan, 2 peaks can be observed as indicated in the plot. The XRR spectrum is not ideal for full spectrum analysis because of lack of additional oscillations. This lack of oscillations is mainly due to the sample flatness and smoothness. As the SEM image indicates, after electro-polishing, there were still significant amount of "valleys" on the sample. However, the oxide thickness is calculated to be 8.3 nm based on these 2 peaks. This result is inconsistent with the 400nm value measured by SEM. This inconsistency is attributed to significant errors originated from the surface roughness associated with the valleys and hills in the electro-polished Pu sample, as illustrated in Figures 4 and 5.

(a) Discussions on XRR measurement for Pu oxide on bulk Pu surface:

(i) absorption factor

In order to further understand the XRR spectrum, calculations on the absorption factor and the transmittance contribution was carried on an assumed 200 nm thick Pu oxide on Pu. The x-ray beam was confined to 16 μm thick and 5 mm wide. The path length and transmittance for an x-ray incident on the sample are shown in Figure 13. The result shows that the major absorption of x-ray is in the very low angle of <1° (2θ) and the transmittance will be very close to zero. However, above 1°, the transmittance goes up from 10% to 80% (transmittance of 1 corresponds to 100%). This result suggests that absorption is not the major factor for the low quality of the spectrum for Pu oxide on Pu.

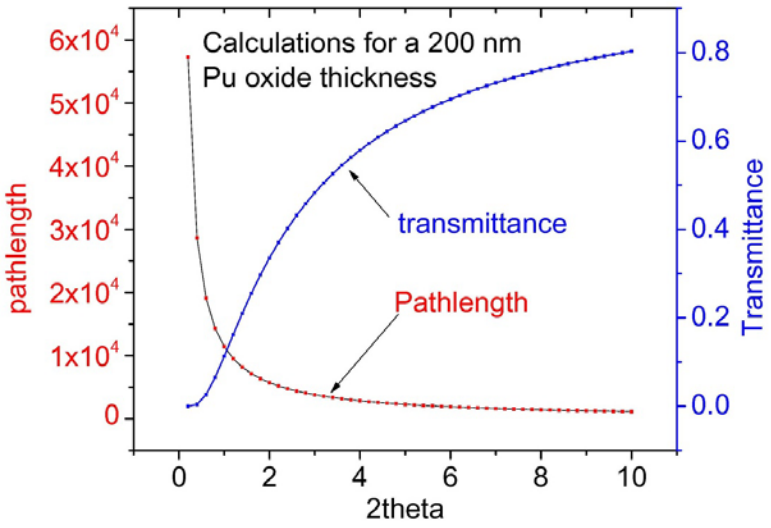

Figure 13: Path lengths and transmittance for a 200 nm thick oxide

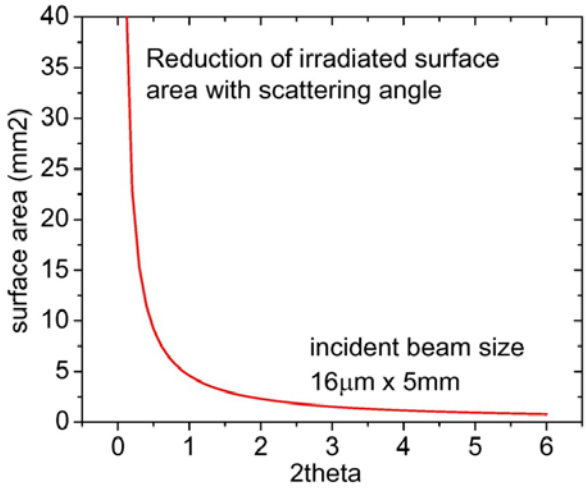

Figure 14: Irradiated surface area on Pu oxide surface

(ii) Changing irradiated surface area

An important factor which affects the resulting spectrum is the changing of the irradiated surface area with scattering angle. Figure 14 shows the calculation for the changing surface area for a beam of 16μm x 5 mm size incident on the sample as a function of scattering angle. As it can be observed, the irradiated surface area drastically decreases to below 5 mm^2 above 1° (2θ) when compared to the area below 1° (2θ). At 6°, for example, the irradiated area is reduced by 85% from that at 1° (2θ).

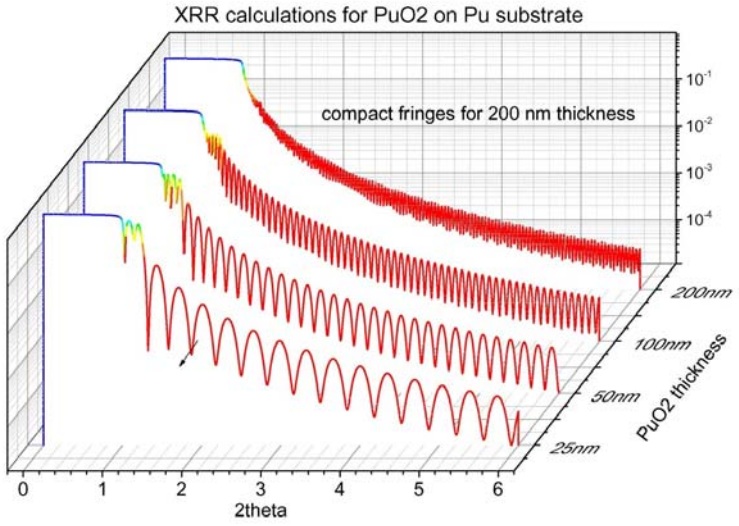

Figure 15: Calculated XRR spectra for Pu oxide on bulk Pu for different oxide thicknesses

(iii) Oxide thickness

Simulations of Pu oxides on bulk Pu surface as a function of film thickness of 25 nm, 50 nm, 100 nm and 200 nm were also carried out and the results are shown in Figure 15. The densities used in the calculation were 11.5 gm/cc, 17 gm/cc for Pu oxide and bulk Pu respectively. The calculation was based on no SR and IR, i.e., assuming perfectly flat. This result clearly demonstrates that the fringes collapse in 2θ with increasing thickness and it would be difficult to detect fringes above 50 nm, limited by instrumental resolution.

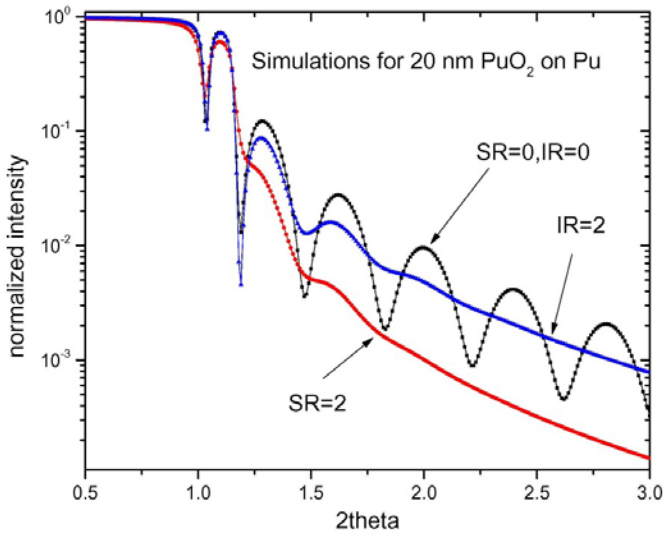

Figure 16: Simulations for 20 nm PuO_2/Pu with different roughness

(iv) Surface and Interface roughness

Surface and interface roughness are very important factors for the success of the XRR experiment since it depends on the interference of the wave from the two scattering planes. Simulations were done with surface roughness of 2 nm and interface roughness of 2 nm for a 20 nm thickness PuO_2 on Pu and is shown in Figure 16 for up to 3 º(2θ). As it can be observed, the number of oscillations dies down very fast with increasing angle. Only 3 peaks can be observed with only 2 nm roughness, hence it can be concluded that the roughness in the PuO_2/Pu sample as shown in Figure 12 was beyond 2 nm.

III. Conclusions and Discussions

XRR technique has been investigated using the recently purchased Rigaku Smartlab instrument. This technique is capable of measuring thin oxide formed on wafers and on bulk metal surface as demonstrated on the test samples of SiO_2 on Si wafer and Ta_2O_5 on bulk Ta. XRR fringes can be observed for both the samples. The oxide thicknesses for SiO_2 on Si wafer were consistent with those measured using the UV-Vis (ultra-violet/visible light spectroscopy) technique.

The XRR fringes of the spectrum from PuO_2/ Pu was not clearly observed from the polished surface. As verified by SEM images, this surface was not smooth enough due to protrusions. Improvements were made by electro-polished resulting in the observation of only 2 fringes in the spectra which was insufficient for proper fitting analysis. This is not surprising because as evidences by the SEM images, there were still significant numbers of "valleys" and "hill" which enhances the unwanted diffuse scattering. Calculation of the thickness based on these peaks was not consistent with the SEM result. Several factors which may contribute to the poor XRR spectrum were discussed. However, the major contributor for this result points towards the inadequate surface roughness of the sample as required for such XRR experiment.

IV. References

[1] Miho Yasaka, *The Rigaku Journal*, 26(2), 2010, 1-9

[2] H. Kiessig, *Ann. Phys.* 10(1931), 715-768

[3] Mirror Reflectivity – Lawrence Berkeley National Laboratory www.henke.lbl.gov/optical_constants/mirrors.html, XRR calculation using the Fresnel equations for a semi-infinite medium

[4] Rigaku propriety software, GlobalFit, Rigaku Corp, USA